ChemComm

COMMUNICATION

View Article Online
View Journal | View Issue

Cite this: *Chem. Commun.*, 2014, **50**, 11903

Received 9th June 2014,
Accepted 18th August 2014

DOI: 10.1039/c4cc04393f

www.rsc.org/chemcomm

Affecting surface chirality *via* multicomponent adsorption of chiral and achiral molecules†

Zongxia Guo,[ab] Inge De Cat,[a] Bernard Van Averbeke,[c] Jianbin Lin,[d] Guojie Wang,‡[a] Hong Xu,[a] Roberto Lazzaroni,*[c] David Beljonne,[c] Albertus P. H. J. Schenning§*[d] and Steven De Feyter*[a]

Here we report on the apparent reduction in surface chirality upon co-assembling a chiral and achiral molecule into a physisorbed self-assembled monolayer at the liquid/solid interface as revealed by scanning tunneling microscopy (STM). Chiral OPV with achiral thymine gives rise to surface-confined supramolecular diastereomers.

The relation between chirality at the molecular scale and supramolecular self-assembly on surfaces has received quite some attention in recent years.[1,2] This interest is fueled by the anticipated impact of surface-assisted self-assembly on the chiral nature of the origin of life and the relevance of surface chirality to materials science. The liquid–solid interface is a promising medium to create surface chirality *via* surface-templated molecular self-assembly, and scanning tunneling microscopy (STM) is a versatile tool to probe the structure of these self-assembled monolayers at the nanoscale.[3,4]

Adsorption of achiral molecules or racemate leads to macroscopically achiral surfaces: individual domains are often 2D chiral though, *i.e.* the molecules assemble into a crystalline lattice that belongs to a chiral plane group (local organisational chirality).[2a,4a] Adsorption of enantiopure molecules leads most often to global organisational chirality: the organization in each domain is identical, and mirror image patterns are not observed.[2a] This does not hold for mono-component systems only but also for bicomponent systems, where one of the components is chiral.

An early exception to the formation of enantiomorphous patterns by the same enantiomer was reported by Walba *et al.*[5] During the monolayer formation of an enantiomer of a liquid-crystalline compound on graphite using STM as a visualization technique, it was observed that heterochiral domains are formed, *i.e.* they are chiral and the mirror image of each other. As these domains are composed of the same enantiomer, these domains must be diastereomeric. About 10 years later, Zhang *et al.* reported a case in which an enantiomer of a 5-alkoxy-isophthalic acid derivative formed mirror image type patterns.[6] This was attributed to a lack of impact of the stereogenic center on the monolayer formation, due to limited molecule–molecule and molecule–substrate interactions at the level of the stereogenic center.

Here, we report on the apparent reduction in surface chirality in multicomponent systems, by self-assembly of a single enantiomer and an achiral co-adsorber at the liquid/solid interface as revealed by means of STM. The bicomponent self-assembly of oligo(*p*-phenylenevinylene) (OPV) derivatives and the achiral co-adsorbing nucleobase, thymine, was investigated at the interface between highly oriented pyrolytic graphite (HOPG) and 1-octanol. The OPV derivatives are functionalized with a diaminotriazine unit with hydrogen-bonding sites complementary to those of thymine (Fig. 1). Ratio dependent experiments and molecular simulation bring insight into the nature of chiral expression and bicomponent self-assembly in general.

To study the nucleobase-assisted self-assembly of OPVs, thymine was premixed with OPVs and the self-assembly of the two building blocks was investigated by STM. Based on the anticipated formation of a 1:1 complex considering the complementarity in hydrogen bonding, solutions including OPV and thymine with a molar ratio of 1:1 were explored at the 1-octanol/HOPG interface. In analogy to those experiments where thymidine was used (Fig. S2 in ESI†),[7] the addition of thymine induced the formation of monolayers with OPV dimer structures instead of initial rosette, *i.e.* the typical supramolecular pattern formed by these OPV derivatives in the absence of a co-adsorber (Fig. 1 and Fig. S1 in the ESI†).[8] Note that this

[a] *Division of Molecular Imaging and Photonics, Department of Chemistry, KU Leuven, Celestijnenlaan 200 F, B-3001 Leuven, Belgium. E-mail: steven.defeyter@chem.kuleuven.be*
[b] *CAS Key Laboratory of Bio-based Materials, Qingdao Institute of Bioenergy and Bioprocess Technology, Chinese Academy of Sciences, Qingdao 266101, China*
[c] *Service de Chimie des Matériaux Nouveaux, Université de Mons, Place du Parc 20, 7000 Mons, Belgium. E-mail: roberto.lazzaroni@umons.ac.be*
[d] *Laboratory of Macromolecular and Organic Chemistry, Eindhoven University of Technology, P.O. Box 513, 5600 MB Eindhoven, The Netherlands. E-mail: a.p.h.j.schenning@tue.nl*

† Electronic supplementary information (ESI) available: STM images and molecular modeling. See DOI: 10.1039/c4cc04393f

‡ Present address: School of Materials Science and Engineering, University of Science and Technology Beijing, No. 30 Xueyuan Road, Beijing 100083, China.
§ Present address: Laboratory of Functional Organic Materials, Eindhoven University of Technology, P.O. Box 513, 5600 MB Eindhoven, The Netherlands.

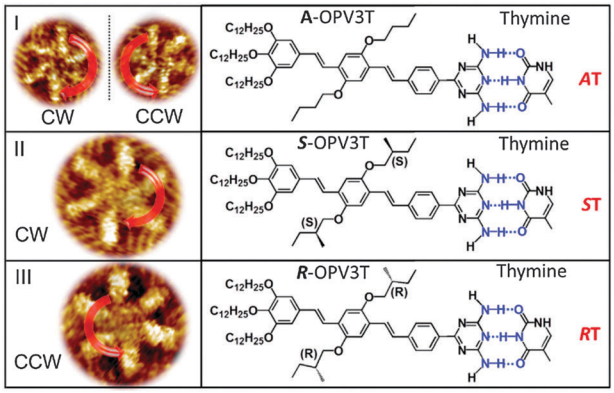

Fig. 1 Molecular structures of *A*-OPV3T, *S*-OPV3T and *R*-OPV3T, and STM images of (I) CW and CCW rosettes from *A*-OPV3T, (II) CW rosettes from *S*-OPV3T, and (III) CCW rosettes from *R*-OPV3T. *AT*, *ST*, and *RT* indicate the complexes of OPV and thymine and corresponding possible formation of complementary H-bonds. The surface-confined supramolecular nanostructures of enantiopure OPVs and OPV–thymidine complexes are shown in Fig. S1 and S2 in the ESI.†

is a rather peculiar case as adding for instance terephthalic acid to di-L-diphenylalanine does not affect the chiral expression at the supramolecular level.[9] The rather broad bright rods correspond to individual OPV units and the faint bright lines between OPV dimer lamellas and parallel to each other are the alkyl chains.[10] Only two out of three alkyl chains per molecule are adsorbed. The other one is probably solvated. Thymine can not be observed as such in the STM images.

The pattern revealed by the STM images is characteristic of the chiral plane group *p*2.[11] As expected, the achiral OPV-derivative forms domains that are related by mirror-symmetry. We label domains arbitrarily as CW or CCW depending on the orientation of dimer rods with respect to the normal on the rows formed by dimers (Fig. 2a and b). Also in the case of the chiral OPV-derivatives, the same type of dimers is observed (Fig. 2c–f). Against expectations, the OPV-enantiomers form CW as well as CCW motifs upon addition of thymine. Such mirror-image related patterns (Fig. 2c *vs.* d; Fig. 2e *vs.* f) can not be enantiomorphous in the strict sense, as they are composed of the same enantiomer. Rather, they are supramolecular diastereomers. It is as if the power of enantiomers to induce surface chirality is weakened by their co-assembly with achiral molecules, leading to an apparent reduction in surface chirality, *i.e.* both CW and CCW dimers are observed for the same enantiomer. To the best of our knowledge, such surface-confined supramolecular diastereomers induced by an achiral molecule have not been reported before.

The unit cell parameters of the patterns are summarized in Table 1. The motifs are labeled according to their composition (*AT*, *RT* or *ST* for *A*-OPV3T–thymine, *R*-OPV3T–thymine and *S*-OPV3T–thymine, respectively) and the handedness (CW or CCW). Unit cell parameters reveal that the CW and CCW motifs of the pure enantiomers are indeed not enantiomorphous; the unit cell parameters differ significantly. *AT*-CW and *AT*-CCW, *ST*-CW and *RT*-CCW, and *ST*-CCW and *RT*-CW are surface-confined supramolecular enantiomers, while the combinations involving the same chiral OPVs are surface-confined

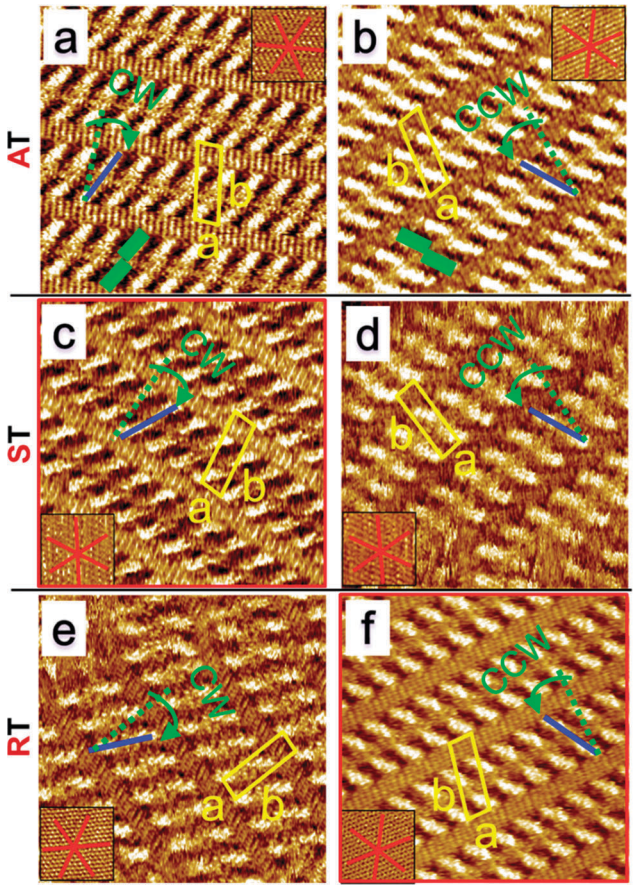

Fig. 2 STM-images of *AT*: (a) CW dimer, I_{set} = 0.6 nA, V_{set} = −0.3 V, (b) CCW dimers, I_{set} = 0.16 nA, V_{set} = −0.11 V, *ST*: (c) CW dimer, I_{set} = 0.1 nA, V_{set} = −0.1 V, (d) CCW dimer, I_{set} = 0.17 nA, V_{set} = −0.23 V, *RT*: (e) CW dimers, I_{set} = 0.16 nA, V_{set} = −0.11 V, (f) CCW dimers, I_{set} = 0.55 nA, V_{set} = −0.29 V. Insets are STM images of the graphite substrate underneath the respective monolayers. The red solid lines reflect the symmetry axes of graphite. Green dotted lines run parallel to the normal of lamella. Solid blue lines show the direction of the OPV dimer long axis. Size of images is 18 × 18 nm^2. [OPV] = [thymine] = 1.0 mM.

Table 1 Unit cell parameters of dimers from *AT*, *ST* and *RT*. Number of images analysed (15 for *AT*, 14 for *ST*, and 16 for *RT*)

	Dimers	*a* (nm)	*b* (nm)	*γ* (°)
AT	CW (47%)	1.81 ± 0.04	4.94 ± 0.09	81 ± 1
	CCW (48%)	1.78 ± 0.03	4.91 ± 0.07	80 ± 1
ST	**CW** (78%)	**1.80 ± 0.02**	**4.94 ± 0.05**	**82 ± 2**
	CCW (10%)	1.97 ± 0.03	4.76 ± 0.06	89 ± 1
RT	CW (10%)	1.95 ± 0.12	4.79 ± 0.10	90 ± 2
	CCW (66%)	**1.80 ± 0.06**	**4.97 ± 0.10**	**83 ± 2**

supramolecular diastereomers (*ST*-CW and *ST*-CCW; *RT*-CW and *RT*-CCW).

Note that equal amounts of CW and CCW dimers are observed for the achiral OPV–thymine combination, as expected. Here, the chiral OPV–thymine mixtures differ, despite the similar experimental conditions in terms of solution composition (concentration and the ratio). Indeed, the ratio of CW and CCW dimers is

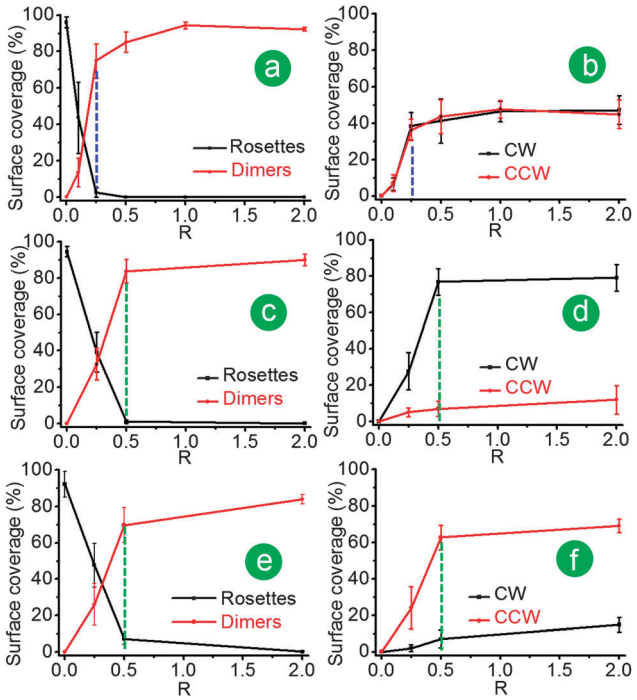

Fig. 3 Molar ratio dependent pattern transformation of *A*T (a), *S*T (c), and *R*T (e) at the 1-octanol/HOPG interface with the addition of thymine. *R* = [thymine]:[OPV]. [OPV] = 1.0 mM. (b), (d), and (f) are the relative amount of CW and CCW dimers as a function of *R*. Dotted blue and green lines in figures indicate the molar ratios where the pattern surface coverage starts to level off for OPV–thymine complex. 20 images (80 × 80 nm^2) were analysed for *A*T, *S*T, and *R*T, respectively.

opposite for the two OPV enantiomers as indicated in Table 1, where the majority structure is indicated in bold. The reason should be sought in the different stability of these dimer structures at the liquid/solid interface, which will be discussed below.

In a next step, we investigated the effect of the solution composition, *i.e.* the ratio (*R*) of thymine *versus* the OPVs. Fig. 3 shows the surface coverage of rosettes and dimers as a function of the solution composition, for a constant concentration of OPV. From the plots, it is clear that with the increase of thymine concentration, rosettes gradually turn into dimers (Fig. S3–S5 in the ESI†). The surface coverage of dimers does not reach 100% because of the existence of some monolayer defects or other motifs that cannot be identified as dimers or rosettes (Fig. S6 in the ESI†).

There are remarkable differences between the achiral and chiral OPVs. For *A*T, about 15% of the surface is covered by dimers at $R = 0.1$ (Fig. S7 in ESI†) and reaches 80% at $R = 0.25$, with an equal amount of CW and CCW dimers (Fig. 3b). For *S*T and *R*T mixtures, the dimer surface coverage reaches also 80%, but only at higher thymine/OPV ratios (~0.5) (Fig. 3d and f). CW dimers are the dominant structures for *S*T and CCW dimers are the dominant ones for *R*T mixtures. Interestingly, the surface coverage of both CW and CCW-type dimers increased simultaneously upon increasing *R* and levels off at about $R = 0.5$. The relative ratio of CW/CCW dimers (~8 : 1 for *S*T) and CCW/CW dimers (~7 : 1 for *R*T) seems to be independent of R.

It is quite striking that such a large fraction of the surface is covered by dimers at very low OPV/thymine ratios. This indicates that dimers are more stable than rosettes. Furthermore, this stabilization must be attributed to the presence of the surface that directs the supramolecular self-assembly. While complex formation in solution for related systems was not observed under conditions that reflect those used for STM imaging.[7] So far, the following conclusions can be drawn: (I) the addition of nucleobase thymine to 1,3-diaminotriazine OPV derivatives induces the pattern transformation from supramolecular rosettes to dimers; (II) *A*T self-assembly gives rise to the appearance of enantiomorphous domains of dimers while each of the combinations of thymine and a chiral OPV, *i.e.* *S*T and *R*T, forms two types of supramolecular dimer arrangements, reflecting surface-confined supramolecular diastereoisomers; (III) *A*T leads to an equal amount of CW and CCW dimer domains, however, in the case of *R*T and *S*T, one diastereomeric dimer motif is favored; (IV) dimer formation is initiated at lower thymine/OPV ratios in the case of *A*T, *i.e.* *A*T complexes are more stable than any of the *S*T or *R*T complexes; (V) in the case of *S*T and *R*T, the ratio of both types of dimers is independent of the thymine/OPV ratio, indicating that their stoichiometry is identical with respect to the co-complexation of thymine, and that the equilibrium constant for the formation of the preferred surface-confined diastereomer is larger.

A Molecular Mechanics/Molecular Dynamics (MM/MD) approach was used to provide an atomistic insight into the supramolecular diastereomer formation, based on energetic considerations. The DREIDING force field,[12] as implemented in the FORCITE tool pack of Materials Studio, was used. The *S*T complex was selected for the simulations; however, the *R*T complex would give the same results except for the relatively different major nanostructures. The simulations show that two OPV molecules and two thymine molecules form one CW or CCW dimer *via* 8 complementary hydrogen bonds (Fig. 4 and Fig. S8 in ESI†). Within the dimers, the H-bond network is made of both 'face-on' thymine–OPV interactions, in which the interacting units are in front of each other, and 'lateral' interactions, in which one NH_2 group on one OPV binds to the thymine molecule in the adjacent pair. In terms of structural models, the CW and CCW dimers are different by the way the chiral groups on the OPV molecules orient with respect to the substrate: in the CW assembly, the most stable structure is with the methyl group on the stereogenic

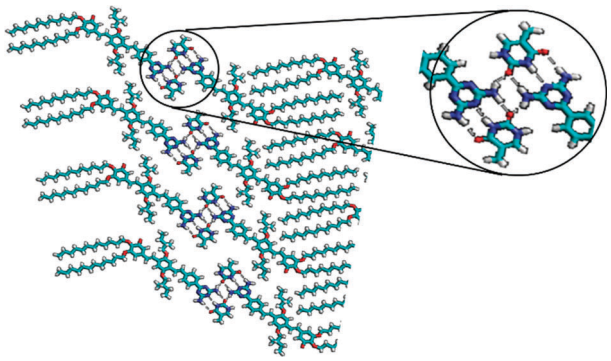

Fig. 4 Simulated models for the monolayer of the CW dimers from *S*T on graphite.

centers of the *S*-OPV molecules directed towards the graphite surface and the ethyl group is pointing away from it, while in the CCW dimers the most stable situation is with the methyl groups pointing upwards (Fig. S9 in ESI†). In terms of stability, a CW dimer is more favourable over its CCW counterpart by about 1.6 kcal mol^{-1}. The energy related to the H-bond system is identical in both assemblies and it is the van der Waals interactions with the surface that are the key factor. In particular, the CW assembly shows 5 CH–π interactions per chiral side group while in the CCW system, only 3 such interactions are present (see Fig. S10 in the ESI†) and this difference is directly related to the different conformation around the stereogenic center. Given that the energy of a CH–π contact is on average 0.8 kcal mol^{-1},[13] the difference in stability between the two assemblies is consistent with the key role of this specific interaction of the chiral groups with the surface.[14]

In conclusion, the impact of an achiral nucleobase (thymine) on the self-assembly of achiral and chiral OPV derivatives was systematically studied by means of STM and force field simulations at the liquid/solid interface. The nucleobase-induced pattern transformation of OPV derivatives from rosettes to dimers was observed. As such, the OPV derivatives ''sense'' the presence of thymine, while achiral OPV derivatives are more ''sensitive'' than chiral ones to the presence of thymine, *i.e.* a transition from rosettes to dimers happens at a smaller thymine to OPV ratio for the achiral derivatives. Quite unexpectedly, surface-confined supramolecular diastereomers were formed in the case of coadsorption of achiral thymine with an enantiopure OPV derivative, in a sense leading to reduction of the degree of surface chirality. This adds to the complexity of multicomponent self-assembly, and provides a way to ''tune'' surface chirality, as it shows that it is not necessary to add the optical antipode molecule to have an impact on surface chirality.

The research leading to these results has received funding from the European Community's Seventh Framework Programme under grant agreement no. NMP4-SL-2008-214340, project RESOLVE. We would also like to thank the Interuniversity Attraction Poles Programme (P7/05) initiated by the Belgian Science Policy Office and the Research Fund of KU Leuven through GOA 11/003, the Fund of Scientific Research – Flanders (FWO), and The Netherlands Organisation for Scientific Research (NWO). We gratefully acknowledge Freek Houben, and Željko Tomović for synthesis of the compounds. We thank E. W. Meijer and David Amabilino for stimulating discussions.

Notes and references

1 (*a*) M. O. Lorenzo, C. J. Baddeley, C. Muryn and R. Raval, *Nature*, 2000, **404**, 376–379; (*b*) R. Fasel, M. Parschau and K.-H. Ernst, *Nature*, 2006, **439**, 449–452; (*c*) S. Weigelt, C. Busse, L. Petersen, E. Rauls, B. Hammer, K. V. Gothelf, F. Besenbacher and T. R. Linderoth, *Nat. Mater.*, 2006, **5**, 112–117; (*d*) S. Haq, N. Liu, V. Humblot, A. P. J. Jansen and R. Raval, *Nat. Chem.*, 2009, **1**, 409–414; (*e*) D. Écija, K. Seufert, D. Heim, W. Auwärter, C. Aurisicchio, C. Fabbro, D. Bonifazi and J. V. Barth, *ACS Nano*, 2010, **4**, 4936–4942; (*f*) T. G. Gopakumar, F. Matino, B. Schwager, A. Bannwarth, F. Tuczek, J. Kröger and R. Berndt, *J. Phys. Chem. C*, 2010, **114**, 18247–18251; (*g*) V. Demers-Carpentier, G. Goubert, F. Masini, R. Lafleur-Lambert, Y. Dong, S. Lavoie, G. Mahieu, J. Boukouvalas, H. Gao, A. M. H. Rasmussen, L. Ferrighi, Y. Pan, B. Hammer and P. H. McBreen, *Science*, 2011, **334**, 776–780; (*h*) N. A. Wasio, R. C. Quardokus, R. P. Forrest, C. S. Lent, S. A. Corcelli, J. A. Christie, K. W. Henderson and S. A. Kandel, *Nature*, 2014, **507**, 86–89.

2 (*a*) S. M. Barlow and R. Raval, *Surf. Sci. Rep.*, 2003, **50**, 201–341; (*b*) K.-H. Ernst, *Curr. Opin. Colloid Interface Sci.*, 2008, **13**, 54–59; (*c*) R. Raval, *Chem. Soc. Rev.*, 2009, **38**, 707–721; (*d*) K.-H. Ernst, *Top. Curr. Chem.*, 2006, **265**, 209–252; (*e*) L. Pérez-Garcia and D. B. Amabilino, *Chem. Soc. Rev.*, 2007, **36**, 941–967.

3 (*a*) F. Stevens, D. J. Dyer and D. M. Walba, *Angew. Chem., Int. Ed. Engl.*, 1996, **35**, 900–901; (*b*) S. De Feyter, A. Gesquière, P. C. M. Grim and F. C. De Schryver, *Langmuir*, 1999, **15**, 2817–2822; (*c*) D. G. Yablon, J. Guo, D. Knapp, H. Fang and G. W. Flynn, *J. Phys. Chem. B*, 2001, **105**, 4313–4316; (*d*) T. Chen, W.-H. Yang, D. Wang and L.-J. Wan, *Nat. Commun.*, 2013, **4**, 1389; (*e*) F. Hu, X. Zhang, X. Wang, S. Wang, H. Wang, W. Duan, Q. Zeng and C. Wang, *ACS Appl. Mater. Interfaces*, 2013, **5**, 1583–1587.

4 (*a*) K. E. Plass, A. L. Grzesiak and A. J. Matzger, *Acc. Chem. Res.*, 2007, **40**, 287–293; (*b*) J. A. A. W. Elemans, I. De Cat, H. Xu and S. De Feyter, *Chem. Soc. Rev.*, 2009, **38**, 722–736; (*c*) N. Katsonis, E. Lacaze and B. L. Feringa, *J. Mater. Chem.*, 2008, **18**, 2065–2073.

5 D. M. Walba, F. Stevens, N. A. Clark and D. C. Parks, *Acc. Chem. Res.*, 1996, **29**, 591–597.

6 J. Zhang, A. Gesquière, M. Sieffert, M. Klapper, K. Müllen, F. C. De Schryver and S. De Feyter, *Nano Lett.*, 2005, **5**, 1395–1398.

7 (*a*) Z. X. Guo, I. De Cat, B. Van Averbeke, J. Lin, G. Wang, H. Xu, R. Lazzaroni, D. Beljonne, E. W. Meijer, A. P. H. J. Schenning and S. De Feyter, *J. Am. Chem. Soc.*, 2011, **133**, 17764–17771; (*b*) Z. X. Guo, I. De Cat, B. Van Averbeke, E. Ghijsens, J. Lin, H. Xu, G. Wang, F. J. M. Hoeben, Ž. Tomović, R. Lazzaroni, D. Beljonne, E. W. Meijer, A. P. H. J. Schenning and S. De Feyter, *J. Am. Chem. Soc.*, 2013, **135**, 9811–9819.

8 (*a*) P. Jonkheijm, A. Miura, M. Zdanowska, F. J. M. Hoeben, S. De Feyter, A. P. H. J. Schenning, F. C. De Schryver and E. W. Meijer, *Angew. Chem., Int. Ed.*, 2004, **43**, 74–78; (*b*) A. Miura, P. Jonkheijm, S. De Feyter, A. P. H. J. Schenning, E. W. Meijer and F. C. De Schryver, *Small*, 2005, **1**, 131–137; (*c*) A. Minoia, Z. X. Guo, H. Xu, S. J. George, A. P. H. J. Schenning, S. De Feyter and R. Lazzaroni, *Chem. Commun.*, 2011, **47**, 10924–10926; (*d*) N. Katsonis, H. Xu, R. M. Haak, T. Kudernac, Z. Tomovic, S. George, M. Van der Auweraer, A. P. H. J. Schenning, E. W. Meijer, B. L. Feringa and S. De Feyter, *Angew. Chem., Int. Ed.*, 2008, **47**, 4997–5001.

9 Y. Wang, M. Lingenfelder, T. Classen, G. Costantini and K. Kern, *J. Am. Chem. Soc.*, 2007, **129**, 15742–15743.

10 (*a*) G. C. Mcgonigal, R. H. Bernhardt and D. J. Thomson, *Appl. Phys. Lett.*, 1990, **57**, 28–30; (*b*) R. Lazzaroni, A. Calderone, J. L. Brédas and J. P. Rabe, *J. Chem. Phys.*, 1997, **107**, 99–105.

11 (*a*) S. B. Lei, C. Wang, S. X. Yin, H. N. Wang, F. Xi, H. W. Liu, B. Xu, L. J. Wan and C. L. Bai, *J. Phys. Chem. B*, 2001, **105**, 10838–10841; (*b*) K. E. Plass, K. Kim and A. J. Matzger, *J. Am. Chem. Soc.*, 2004, **126**, 9042–9053.

12 S. L. Mayo, B. D. Olafson and W. A. Goddard, *J. Phys. Chem.*, 1990, **94**, 8897–8909.

13 K. Shibasaki, A. Fujii, N. Mikami and S. Tsuzuki, *J. Phys. Chem. A*, 2006, **110**, 4397–4404.

14 K.-H. Ernst, *Phys. Status Solidi B*, 2012, **249**, 2057–2088.

